

A. N. GODWIN

**Three dimensional pictures for Thom's parabolic umbilic**

*Publications mathématiques de l'I.H.É.S.*, tome 40 (1971), p. 117-138

[http://www.numdam.org/item?id=PMIHES\\_1971\\_\\_40\\_\\_117\\_0](http://www.numdam.org/item?id=PMIHES_1971__40__117_0)

© Publications mathématiques de l'I.H.É.S., 1971, tous droits réservés.

L'accès aux archives de la revue « Publications mathématiques de l'I.H.É.S. » (<http://www.ihes.fr/IHES/Publications/Publications.html>) implique l'accord avec les conditions générales d'utilisation (<http://www.numdam.org/conditions>). Toute utilisation commerciale ou impression systématique est constitutive d'une infraction pénale. Toute copie ou impression de ce fichier doit contenir la présente mention de copyright.

NUMDAM

Article numérisé dans le cadre du programme  
Numérisation de documents anciens mathématiques  
<http://www.numdam.org/>

# THREE DIMENSIONAL PICTURES FOR THOM'S PARABOLIC UMBILIC

by A. N. GODWIN

## 1. Introduction.

Thom [3] has introduced the seven elementary catastrophes in  $\mathbf{R}^4$ . The most complicated and perhaps the most interesting of these is the last in Thom's list, which he calls the parabolic umbilic. In his book [3] and papers [1, 2] he has drawn some qualitative sketches of some two dimensional sections of the surface used in applications of the theory. Here we give more accurate pictures of this surface based on quantitative computer analysis.

The parabolic umbilic is given by the formula

$$(1) \quad V = x^2y + y^4 + ty^2 + wx^2 - ux - vy$$

where we consider  $V$  as a potential function

$$V : \mathbf{R}^4 \times \mathbf{R}^2 \rightarrow \mathbf{R}$$

with  $c = (u, v, w, t) \in \mathbf{R}^4$  a point in the unfolding (or control [5]) space and  $(x, y)$  as points in the state space  $\mathbf{R}^2$ . For each  $c \in \mathbf{R}^4$  we have a potential function

$$V_c : \mathbf{R}^2 \rightarrow \mathbf{R}$$

and for each  $c$  we are interested in stationary points of  $V_c$ . Most (open dense)  $c \in \mathbf{R}^4$  give rise to  $V_c$  with isolated non degenerate stationary points and such  $c$  are called *regular points*, the remaining points belong to the *bifurcation set*,  $B \subset \mathbf{R}^4$  corresponding to those potentials which have coincidences amongst their stationary points. The main objective of this paper is to analyse  $B$  and to draw the intersections of  $B$  with the four three-dimensional coordinate hyperplanes of  $\mathbf{R}^4$ .

The secondary objective is to draw the *Maxwell set* which we now define. In each component of  $\mathbf{R}^4 - B$  there are 0, 1 or 2 minima and 0 or 1 maxima (saddle points being ignored). The Maxwell convention assigns a preference to the lower minimum if more than one exist. So in those components with two minima we pick out the set of points representing  $V_c$  with two equal minima as the Maxwell set. In applications the *catastrophe set* is important, since this is the set representing possible discontinuities

in space-time. The catastrophe set comprises two types of point; (i) those points of the set B which separate regions that differ by one in the number of minima; (ii) (in some applications) the Maxwell set; and so can be deduced from our diagrams.

## 2. Two dimensional sections of B.

Stationary points of (1) are given by

$$\frac{\partial V}{\partial x} = \frac{\partial V}{\partial y} = 0$$

and the set B is given by two stationary points coincident, this being defined by the equation

$$\begin{vmatrix} \frac{\partial^2 V}{\partial x^2} & \frac{\partial^2 V}{\partial x \partial y} \\ \frac{\partial^2 V}{\partial x \partial y} & \frac{\partial^2 V}{\partial y^2} \end{vmatrix} = 0$$

i.e. Hessian vanishes. Thus we have 3 equations

$$(2) \quad u = 2x(y + w)$$

$$(3) \quad v = x^2 + 4y^3 + 2ty$$

$$(4) \quad x^2 = (y + w)(6y^2 + t)$$

and the set B is given explicitly by elimination of  $x, y$ . This can be written as

$$(5) \quad u^2 = 4(p + w)^3(6p^2 + t)$$

where

$$(6) \quad p = \sqrt[3]{\{(v/8 - u^2/32) + \sqrt{[(u^4/16 - u^2v/2 + v^2)/16 + t^3/54]}\}} \\ + \sqrt[3]{\{(v/8 - u^2/32) - \sqrt{[(u^4/16 - u^2v/2 + v^2)/16 + t^3/54]}\}},$$

or other two roots of the cubic equation (8), so that B appears to consist of 3 parts. The form (5), (6), is however not very easy to use in calculations and so we have used the form

$$(7) \quad u = 2[(y + w)^3(6y^2 + t)]^{1/2}$$

$$(8) \quad v = 10y^3 + 6wy^2 + 3ty + wt$$

which for given  $w, t$  is a pair of parametric equations in parameter  $y$  for a curve in the  $u, v$  plane.

The equations (7), (8) can be seen to give real pairs  $(u, v)$  for those values of  $y$  for which the quintic expression  $(y + w)^3(6y^2 + t)$  is positive, so we can write down ranges of  $y$  relevant to B for any given  $w, t$ . Further we can see that the curve will have reflective symmetry in the  $v$ -axis. Also in general case we can consider large  $y$

and we have (i)  $y \rightarrow -\infty$  no real points (ii)  $y \rightarrow +\infty v \sim u^{6/5}$ . For the more detailed analysis of B that follows, we need besides (7) and (8) the equations

$$(9) \quad \frac{dv}{dy} = 30y^2 + 12wy + 3t$$

$$(10) \quad \frac{du}{dy} = \sqrt{[(y+w)/(6y^2+t)](30y^2+12wy+3t)}$$

(taking positive square root and looking at  $u \geq 0$ ) which apart from exceptional points gives

$$(11) \quad \frac{dv}{du} = \sqrt{[(6y^2+t)/(y+w)]}.$$

We shall further require the expression

$$(12) \quad \frac{d}{dy} \left( \frac{dv}{du} \right) = (6y^2 + 12wy - t) / 2(y+w)^{3/2}(6y+t)^{1/2}$$

the positive square roots applying to  $u \geq 0$ . Using (7)-(12) we can decide the ranges of values of  $y$  for each  $(u, v)$  graph and choose suitable  $w, t$  values to capture the four dimensional behaviour of B. Further these formulae give a basis for establishing such features as cusps, discontinuities and intersections which need analytic support for computer evidence.

To get at the details of  $u, v$  sections we split the discussion into the three cases  $t > 0, t = 0, t < 0$ .

(I)  $t > 0$ . — For  $t > 0$  we see from (7) that the range of  $y$  for which real points occur is the semi-infinite interval  $y \geq -w$ , the quintic for  $u$  having a triple real root at  $y = -w$  and two complex roots. From (9), (10), (11) we see that points of interest are  $y = -w, y = \pm \sqrt{(-t/6)}$  and  $y = -w/5 \pm \sqrt{(w/25 - t/10)}$ . The points  $y = \pm \sqrt{(-t/6)}$  correspond to imaginary  $u$  and we do not consider them further here.  $y = -w$  gives  $u = 0, v = -4w^3 - 2tw$  and by using (i)  $\lim_{y \rightarrow -w} (dv/du) = +\infty$ ; (ii) symmetry; we see that we have a cusp on the  $v$ -axis, pointing in the  $v$  decreasing direction. This will hold for all  $w$ .  $y = -w/5 \pm \sqrt{[w^2/25 - t/10]}$  is real for  $w^2 \geq 5t/2 (> 0)$ , but for such negative  $w$  we have

$$-w/5 \pm \sqrt{[w^2/25 - t/10]} < -2w/5 < -w$$

so that these  $y$  values give imaginary  $u$ . Thus we need only consider  $w \geq \sqrt{[5t/2]}$ , and since for such  $w$

$$(13) \quad -w < -w/5 - \sqrt{[w^2/25 - t/10]} \leq -w/5 + \sqrt{[w^2/25 - t/10]} < 0$$

these points do not complicate the picture at  $y = -w$ .

Now from (11)  $dv/du > 0$ , except for perhaps exceptional points, these being just the points where  $dv/du$  is undefined due to the vanishing of  $30y^2 + 12wt + 3t$  i.e.

$y = -w/5 \pm \sqrt{[w^2/25 - t/10]}$ . At these points  $du/dy$  and  $dv/dy$  both vanish giving a cusp point in the  $u, v$  curve. (12) shows that  $dv/du$  is decreasing with  $y$  for

$$-w - \sqrt{[w^2 + t/6]} < y < -w + \sqrt{[w^2 + t/6]}$$

and since for  $w > 0$ ,

$$-w - \sqrt{[w^2 + t/6]} < -w < 0 < -w + \sqrt{[w^2 + t/6]},$$

$dv/du$  decreases through both cusps (compare (13)) so that branches are on opposite sides of the common tangent. To establish that picture is always as given in Fig. 7 (inset  $w = 0.707$ ) or Fig. 11 (insets  $t > 0$ ) we need only consider the  $u$ -values corresponding to the  $v$ -value given by  $y = -w/5 - \sqrt{[w^2/25 - t/10]}$  and these are calculated as the cusp point and the point given by  $y = -w/5 + 2\sqrt{[w^2/25 - t/10]}$  (by use of (8)). Letting  $y = (-w/5 + a)$  we find

$$(14) \quad u = 24[a^5 + 2wa^4 + (w^2 + t/6)a^3 - 4w(w^2/25 - t/10)a^2 - \{16w^2(w^2/25 - t/10)/5\}a + 32w^3(2w^2/25 + t/3)/125]$$

and by putting  $a = -\sqrt{[w^2/25 - t/10]}$  and  $a = +2\sqrt{[w^2/25 - t/10]}$  we will get the  $u$ -values on the  $v = \text{const.}$  line. The difference in  $u$ -values, the cusp point being assumed smaller, is given by

$$(15) \quad \Delta(u^2) = 18.24 \cdot b^4 \cdot (w + b)$$

where  $b = \sqrt{[w^2/25 - t/10]}$ . Since  $\Delta(u^2) > 0$  for all  $t > 0$ ,  $w > 0$ , the point on the same  $v$ -level as the cusp is outside the cusp and this is sufficient to confirm the diagrams. The  $(y, w)$  information for  $t > 0$  is summarised in Fig. 1, this being the key diagram for computer calculations showing range of  $y$  to be searched and relevant  $w$ -values. The results of computer calculations have then been used to construct Fig. 7 and some  $t > 0$  results used in other diagrams.

(II)  $t = 0$ . — For  $w > 0$  we have the  $(u, v)$  graphs modified from the  $t > 0$ ,  $w > \sqrt{[5t/2]}$  case by the drawing together of the lower cusp and its reflection to form the “beak to beak” configuration, Fig. 6 ( $w = 0.5$  inset). This form is predicted by use of (9) and (10) to show that  $y = 0$ ,  $-2w/5$  are cusps, (12) to show  $dv/du$  changes to give a two sided cusp at  $-2w/5$  and a one sided cusp at  $y = 0$ . (15) is then used as in the  $t > 0$  case to show that the  $y = 2w/5$  cusp is inside the curve going to infinity. (11) then shows using the limit as  $y \rightarrow 0$  that  $v = 0$  is tgt to the cusp at  $(0, 0)$  which completes the demonstration. The point given by  $y = -w$  is as in  $t > 0$ , a downward cusp.

With  $t = w = 0$  there is now only the problem of point  $u = v = 0$  which by consideration of (11) can be seen to have  $v = 0$  as a tangent line to the curve, so we have a parabola like curve.

In the case  $w < 0$  we have no real cusp points for  $y = -2w/5$  and  $y = 0$  is a real isolated point. The  $y = -w$  point is a downward cusp.

In Fig. 2 we give the  $(y, w)$  diagram showing ranges and important values of  $y$

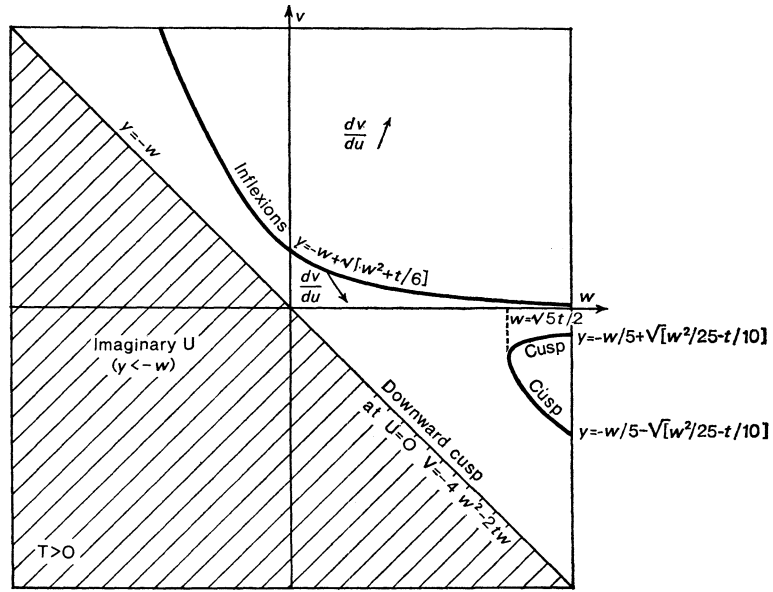


FIG. 1

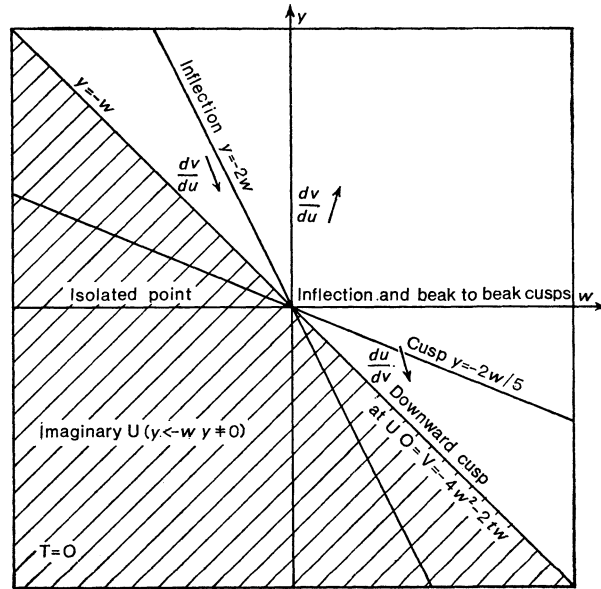


FIG. 2

for any  $w$  when  $t=0$ , the computer calculated  $u, v$  sections have been used to construct Fig. 6.

(III)  $t < 0$ . — From (7) we see that in this case there can be two ranges of  $y$  that give real  $u$ , one range being a finite interval giving rise to a bounded part of the  $(u, v)$  curve, the other a semi-infinite interval corresponding to curves studied in (I) and (II).

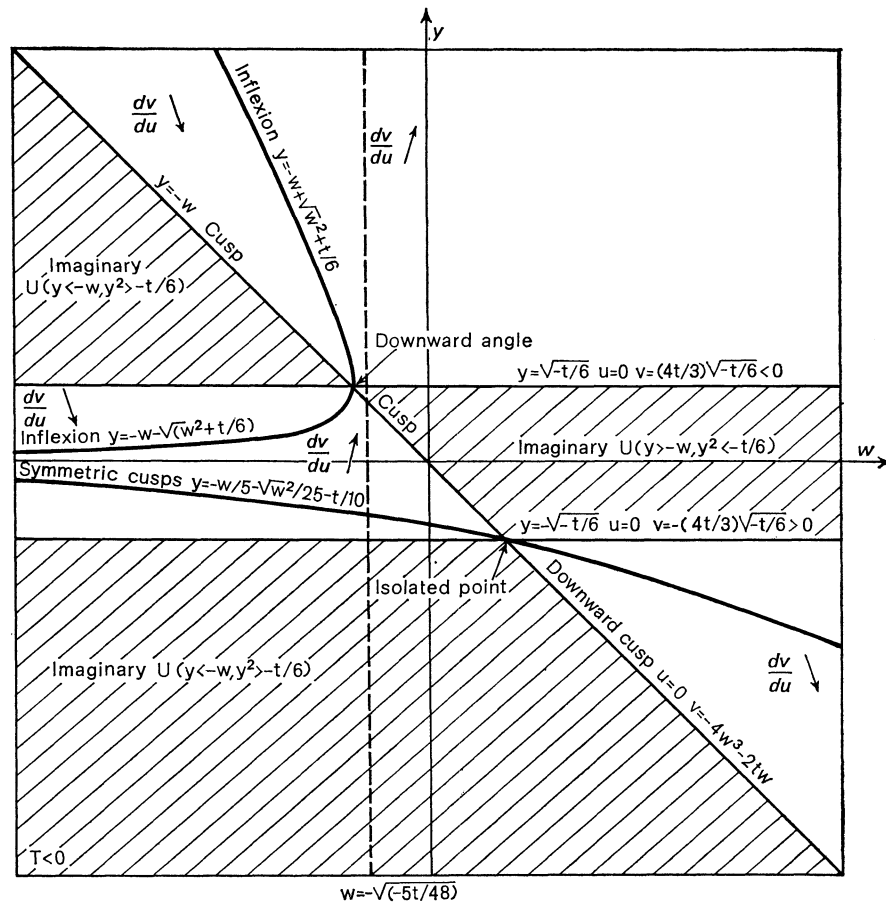


FIG. 3

The end points of these  $y$  ranges depend for each fixed  $t$  on  $w$  and can be seen clearly in the  $(y, w)$  diagram Fig. 3 as straight lines. At the end points of these  $y$ -intervals  $u=0$  and  $v$  will be given by  $-4w^3 - 2tw, \pm(4t/3)\sqrt{[-t/6]}$ . These  $(v, w)$  curves for fixed  $t$  are given in Fig. 4, a cubic with two horizontal tangent lines.

Using results summarised in Fig. 3, 4 and considering  $dv/du$  we know the general form of the curve for each  $w, t$  but certain features need more detailed analysis. These features are: types of intersection with axis of symmetry  $u=0$ ; possible cusps; possible double points.

The downward cusp of (I) and (II) will occur at  $y = -w, v = 4w^3 - 2tw$  and

the horizontal,  $v = \text{const.}$  tangent, will occur at the other two points  $y = \pm\sqrt{[-t/6]}$ ,  $v = \pm(4t/3)\sqrt{[-t/6]}$  except in cases of coincidence amongst these  $y$  values. This can be proved by using limits of  $dv/du$  given by (11). If  $w = -\sqrt{[-t/6]}$  then use of (11) shows that the downward cusp becomes a finite angle,  $2 \tan^{-1}(\sqrt{[-12w]})$  bisected by the  $v$ -axis. This point is called a *hyperbolic point* since as  $w$  increases through  $w = -\sqrt{[-t/6]}$  we get in the neighbourhood of the intersection for the finite part the

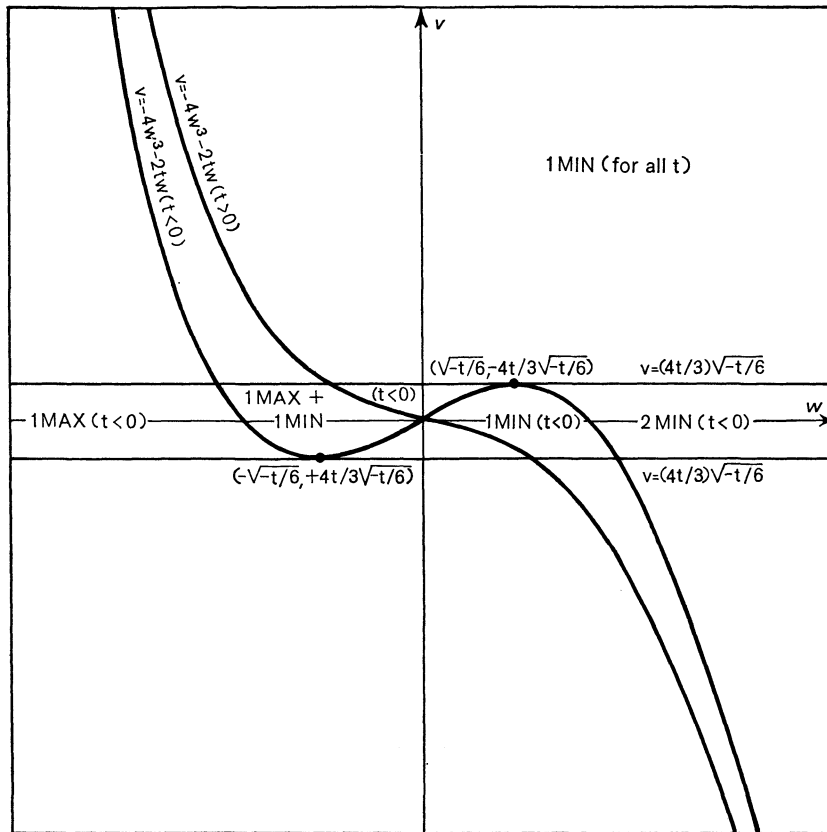


FIG. 4

transition curve  $\rightarrow$  angle  $\rightarrow$  cusp and for the unbounded branch the opposite sequence (cf. Zeeman [4]). For the other possible coincidence  $w = \sqrt{[-t/6]}$  the bounded part of the curve becomes a distinct isolated point  $(0, 8w^3)$ , this point will be called an *elliptic point* since locally the finite part of the curve is Thom's elliptic umbilic.

(9), (10) again give possible cusps at  $y = -w/5 \pm \sqrt{[w^2/25 - t/10]}$  and where this correspond to real  $u$ , these values are marked on Fig. 3. Using this diagram or obvious inequalities of type used in (I) and (II) we can establish that bounded part of curve will have the one real cusp at  $y = -w/5 - \sqrt{[w^2/25 - t/10]}$  except at the elliptic point. (This, of course, becomes two real cusps by reflection in the  $v$ -axis.) (12) shows that for  $w < -\sqrt{[-t/6]}$  there are two inflexion points given by  $y = -w \pm \sqrt{[w^2 + t/6]}$  and no inflexions for other  $w$ . These  $y$  values have been drawn on Fig. 3 and this shows



clearly that one inflexion is on the bounded part of the curve and one on the unbounded section. The computer drawings of each branch can thus be completely interpreted since (11) and results quoted so far show that the finite and unbounded parts cannot separately produce a double point. Taken together, however, a double point can appear as an intersection of the bounded and unbounded parts of the  $(u, v)$  curve. For  $-\sqrt{[-t/6]} \leq w \leq \sqrt{[-t/6]}$  use of (11) and (12) is sufficient to show that intersection occurs only when cusp of finite part is outside the other branch and using (15) to compare  $u$  values we see that this happens for  $w < -\sqrt{[-5t/48]}$ , the cusp point actually being on the other branch at  $w = -\sqrt{[-5t/48]}$ . For  $w > \sqrt{[-t/6]}$ , using (15) and gradient inflexion reasoning we have cusps inside and get transverse intersection for  $w \geq 2\sqrt{[-t/6]}$ , see Fig. 5. For  $w < -2\sqrt{[-t/6]}$  we get no double points. For  $w = -2\sqrt{[-t/6]}$  we have a double point on the axis at  $(0, (-4t/3)\sqrt{[-t/6]})$ . The remaining range of  $w$  is  $(-2\sqrt{[-t/6]}, -\sqrt{[-t/6]})$  which from computer drawings should have one double point and to prove that this is so, formulae so far considered are not sufficient. But formulae and gradient inflexion arguments work for  $w = -\sqrt{[-t/6]}$  and by implicit differentiation

$$(16) \quad \left. \frac{\partial v}{\partial w} \right|_{u=\text{const}} = -2(6y^2 + t)$$

for  $y \neq -w/5 \pm \sqrt{[w^2/25 - t/10]}$  so that for any given  $u$  the unbounded part moves upwards as  $w$  decreases and the bounded part moves downwards. Thus the unbounded part remains between the cusps and only intersects as given by the computer drawn graphs.

### 3. State Space, Component Types and Maxwell Set.

Since the components of  $\mathbf{R}^4 - \mathbf{B}$  contain only potentials with same number and type of stationary points we may define the type of each component by its set of stationary points. Given a point in  $\mathbf{R}^4 - \mathbf{B}$  we may ascertain its type by first solving (7) and (8) for stationary points  $(x, y)$  and then use the Hessian at these points to classify them. Since only one point for each component is required to label the regions of the 3 dimensional pictures, calculations were done for various  $w$  and  $v$  with  $u=0$  and  $t=-6$ . Sufficient points were chosen so that all regions of the three dimensional pictures in Fig. 5-16 could be labelled. These calculations showed that it was possible to have the following stationary sets — 1 saddle point, 1 minimum and 2 saddle points, 2 minima and 3 saddle points, 1 maximum and 2 saddle points or 1 maximum, 1 minimum and 3 saddle points, the quintic equation for stationary point  $x$  values confirming the upper limit of 5 points in these patterns. Since the saddle points are not used in the applications of the theory, only the proper stationary points are referred to in the diagrams.

Zeeman has pointed out to me that turning the potential upside down will interchange maxima and minima which might be useful in some applications. This changed situation can, of course, be easily read off the diagrams presented in this paper. In

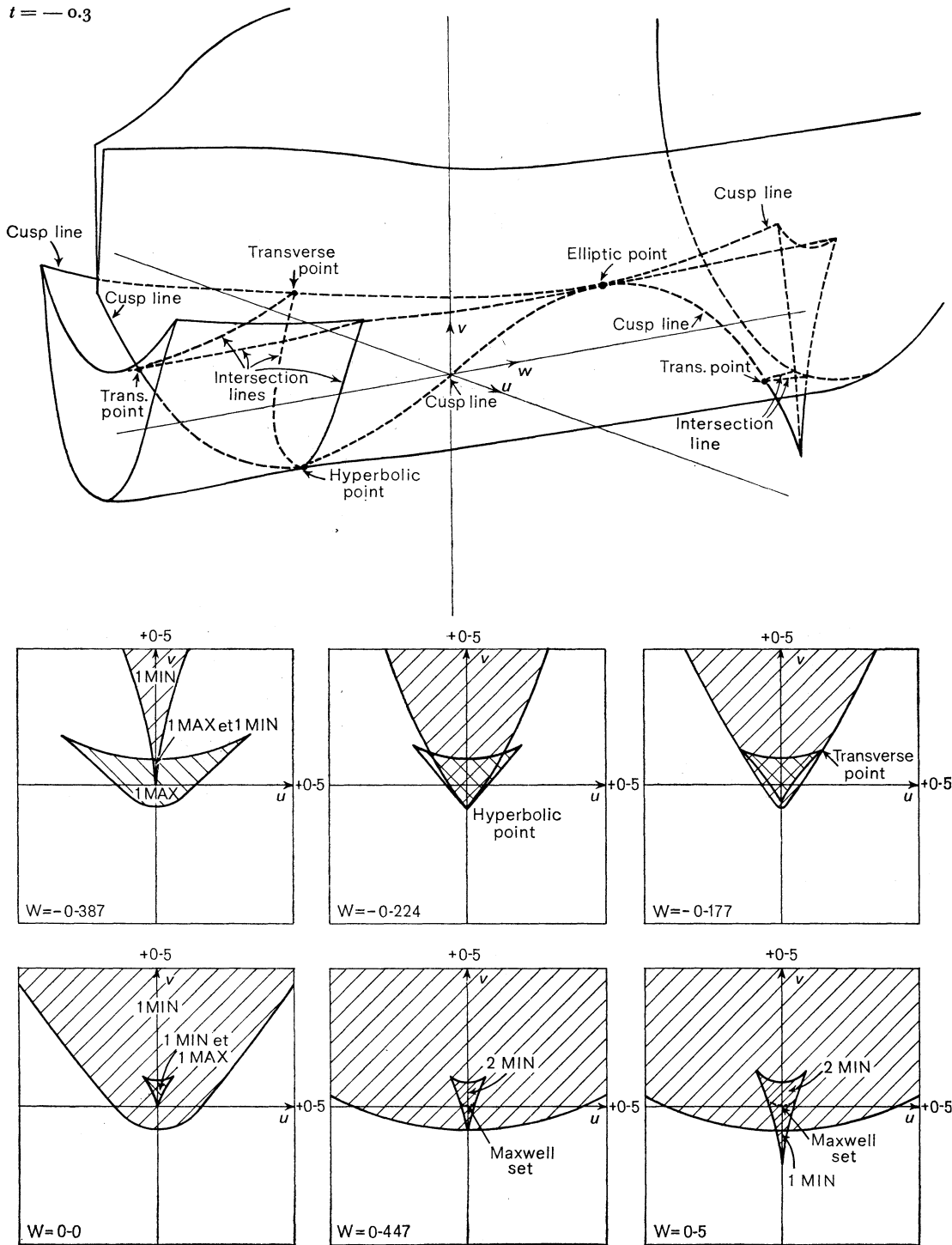


FIG. 5

$t = 0.0$

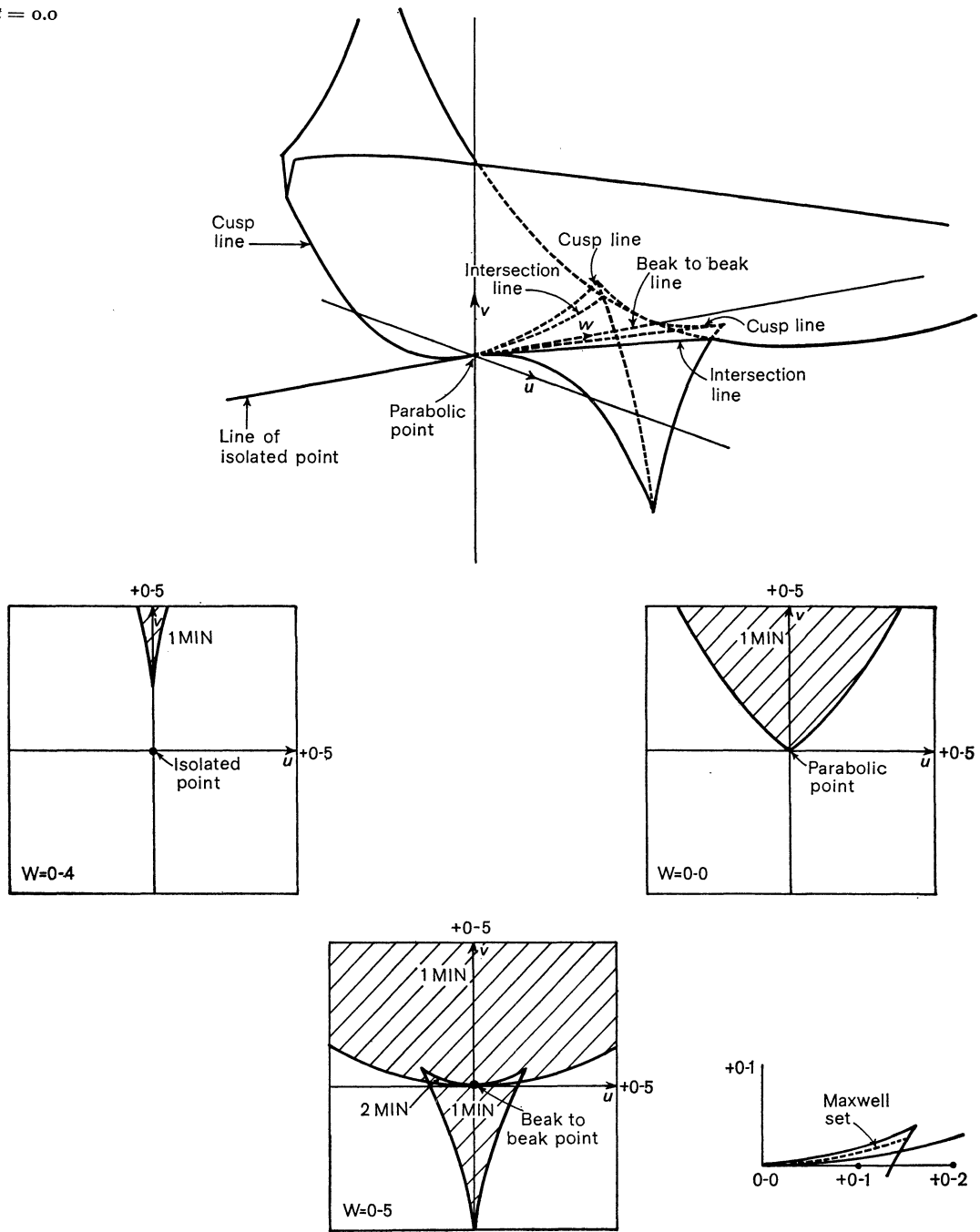


FIG. 6

$t = 0.05$

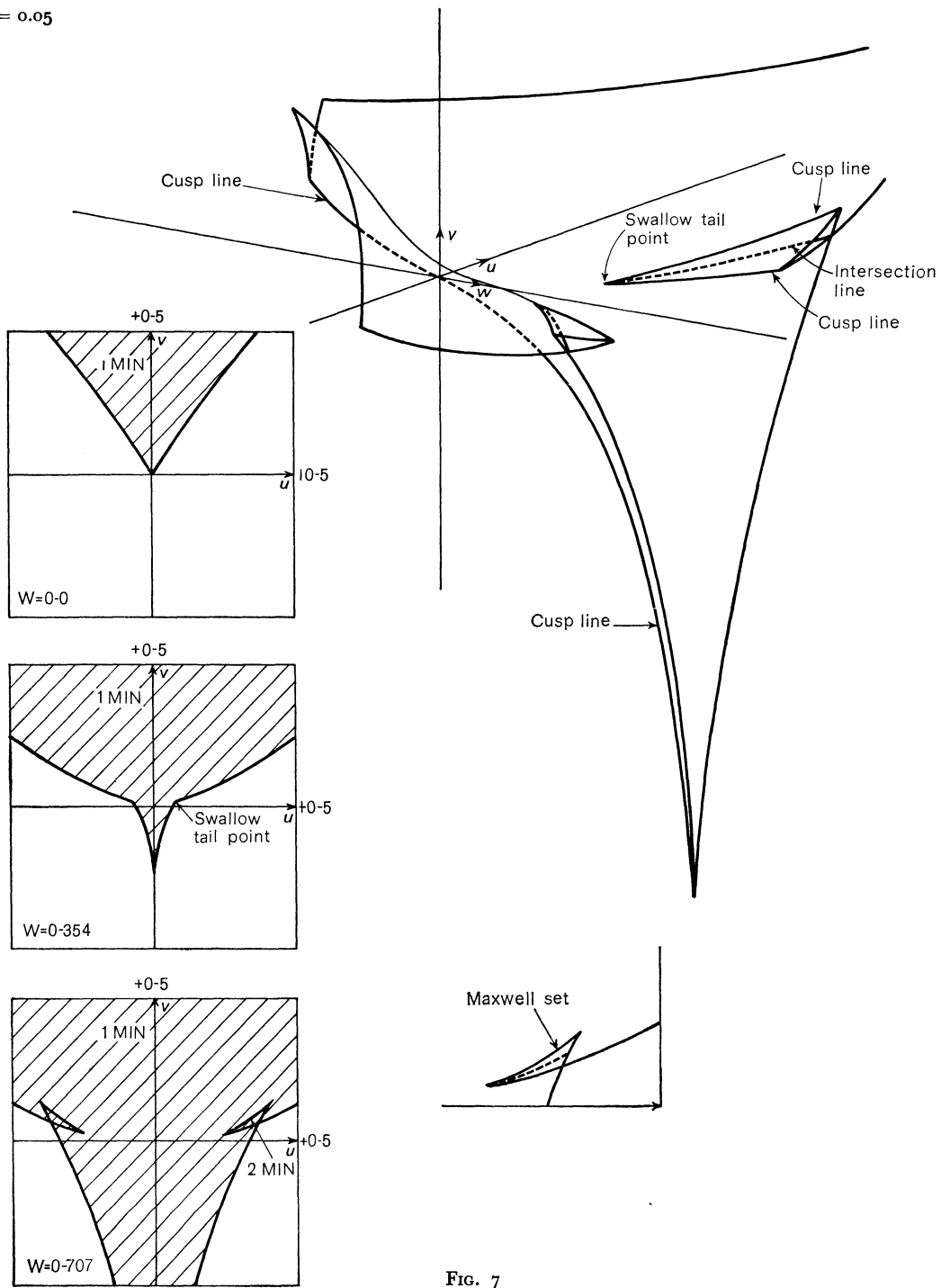


FIG. 7

fact, to relate most closely to the hyperbolic and elliptic umbilic where there can only be one attractor state, we should look at the present pictures this way round.

We are thus in a position to find from the figures the points of the catastrophe set which also are part of B.

To find the Maxwell set, which was defined in § 1, we need further calculations in the region of  $\mathbf{R}^4 - B$  with 2 minima. A computer program was written to scan this component for a fixed  $w$ , since as can be seen from Fig. 11, this case will give a good indication of its behaviour. The outputs from the program were the details of the values, positions and types of the stationary points for each relevant value of  $t, u, v$ . To keep computing time low, a fairly large mesh was used and interpolation for Maxwell set done by hand. The results of these fairly rough calculations are indicated on the relevant inset figures with diagrams of § 4.

**4. Diagrams.**

The first set of diagrams, in Fig. 4-7, give 3 dimensional pictures of sections of B by hyperplanes  $t = \text{const}$ . Fig. 4 is a "control" diagram for Fig. 5-7 showing that these figures can be roughly summarised by the behaviour of the cubic curves

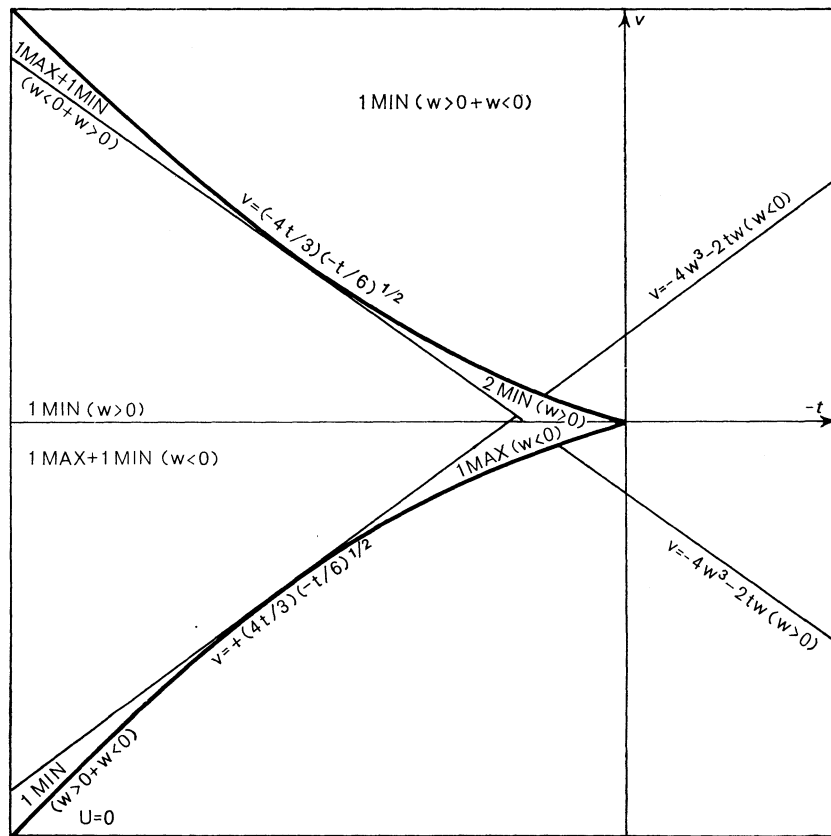
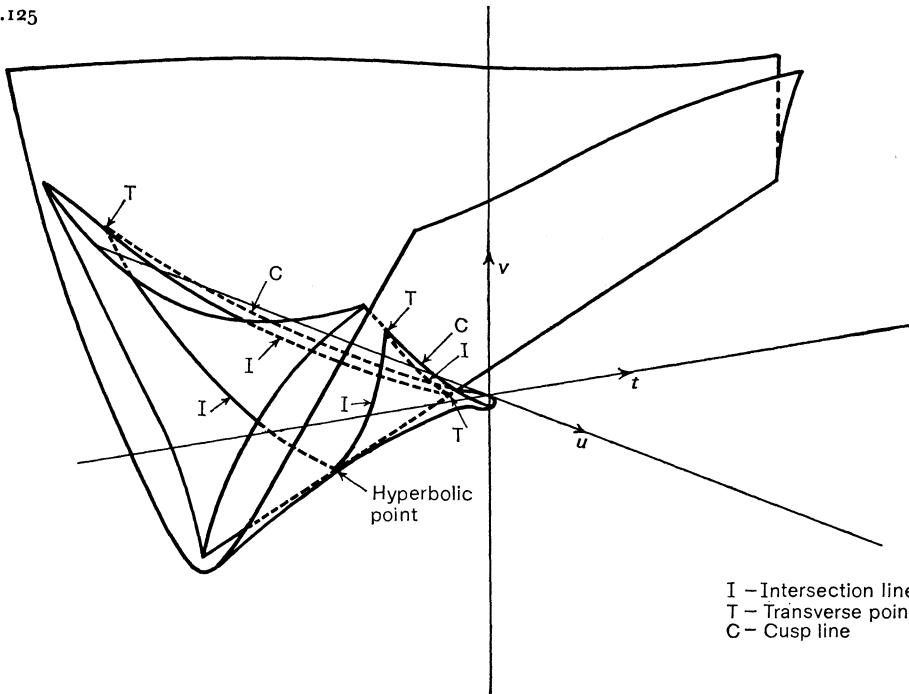


FIG. 8

$w = -0.125$



I - Intersection line  
 T - Transverse point  
 C - Cusp line

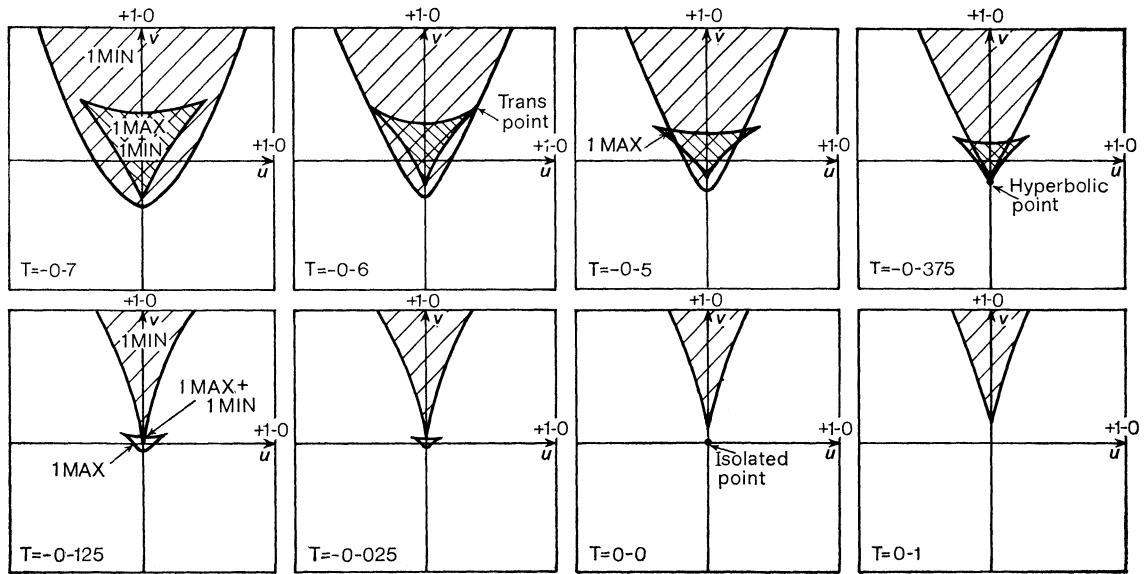


Fig. 9

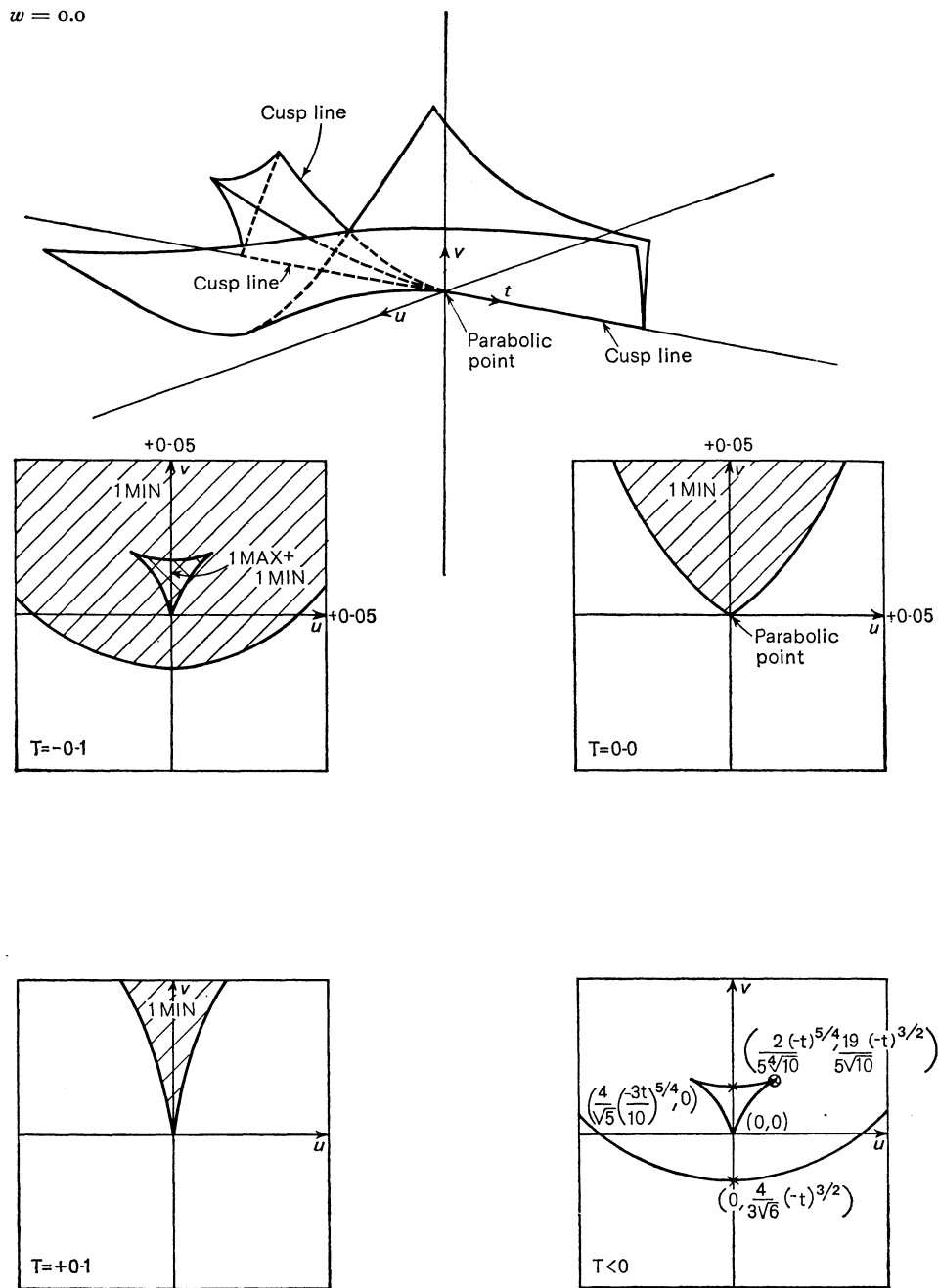


FIG. 10

$w = 0.25$

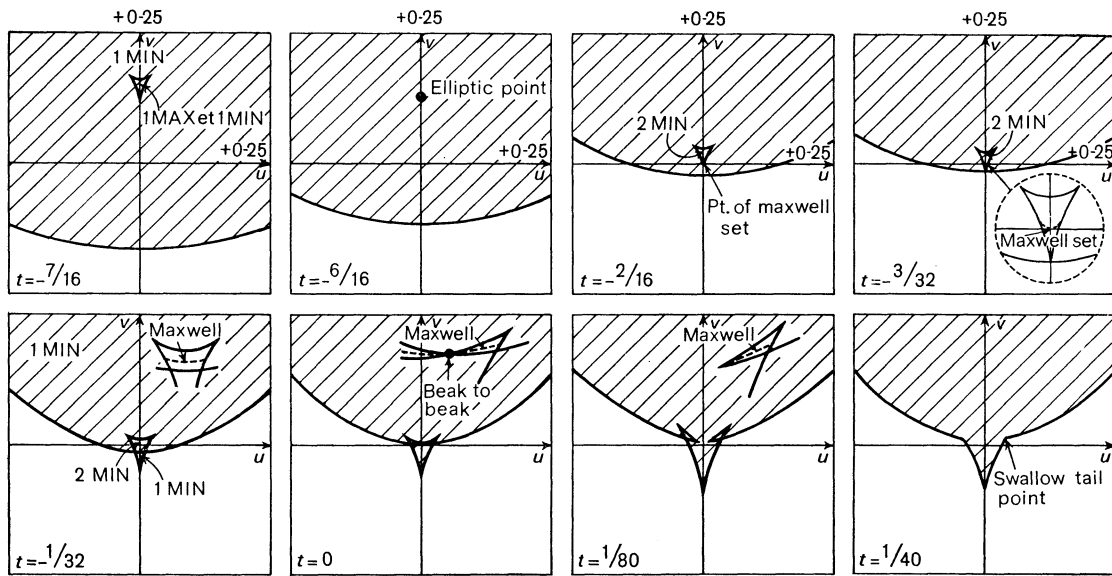
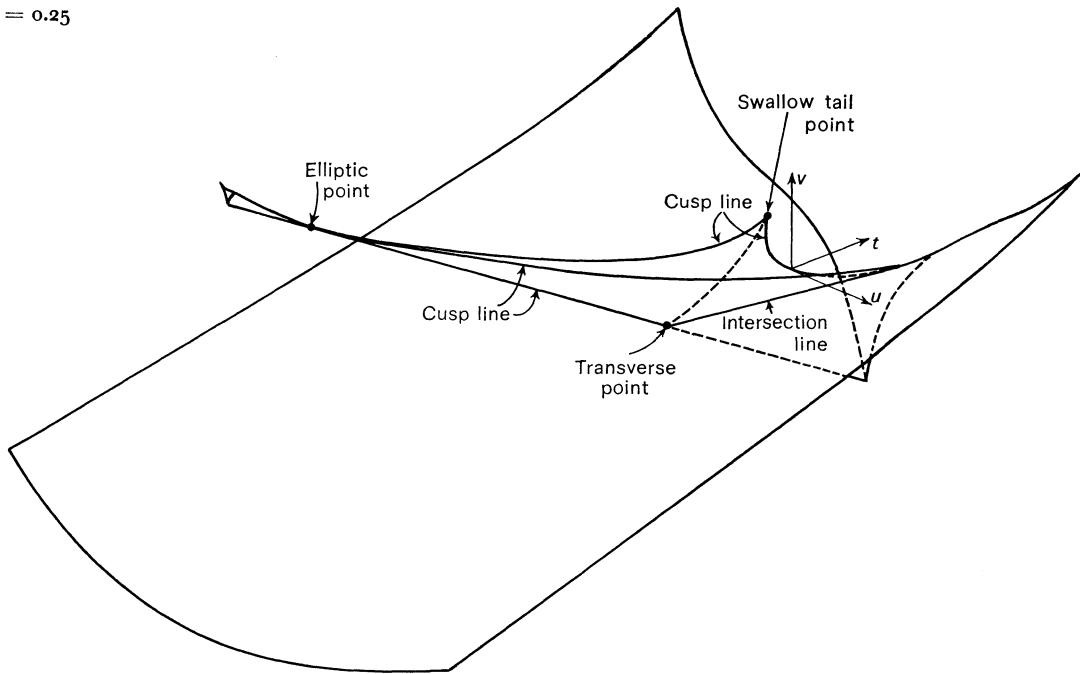


FIG. 11



$v = -4w^3 - 2tw$ . The three types of configuration for the three dimensional section are (i) any  $t < 0$ , (ii)  $t = 0$ , (iii) any  $t > 0$ . The particular choices of  $t = -0.3$  for (i) and  $t = 0.05$  for (iii) were made for reasons of relative scale of feature.

On the three dimensional pictures the labels concentrate on geometric features such as cusp edges, lines of intersection of different parts of B and some special points. Of these special points the elliptic and hyperbolic points have already been defined in § 2. The *parabolic point* then seems a natural name for the origin of coordinates. The name *swallow-tail point* has been given to a pair of points because of the similarity of three dimensional neighbourhoods to one of simpler catastrophe diagrams, Thom [3]. Further certain *transverse points* where a cusp edge cuts another part of B have been indicated. The two dimensional inset diagrams include the component type information and the Maxwell set and are sections of the three-dimension diagram in the same figure. Some of the special points have also been indicated to aid tying together the main diagram with its sections. The inset  $(u, v)$  diagrams are copies of computer drawn diagrams which together with the analysis of § 2 were used in visualising the three-dimensional surfaces. To get some idea of the four-dimensional B we can consider the "controlling" cubic varying with  $t$ .

The next set of diagrams Fig. 8-11 are arranged on the same basis as the first set of diagrams Fig. 4-7 except that  $w$  is now the fourth missing variable and  $t$  is included in the pictures. The "control" diagram is now Fig. 8, the fixed curve  $v = \pm(4t/3)\sqrt{-t/6}$  with a variable tangent line. In Fig. 10 ( $w = 0$ ) the results of extra analysis, showing when turned into pictures, that finite part of the  $(u, v)$ -section flattens out at  $t \rightarrow 0$  is summarised in a general  $t < 0$  section. Otherwise insets and main diagrams are related as described above.

The next pair of diagrams Fig. 12, 13 look at B with  $u$  the missing variable, but here Fig. 13 is obtained by perturbation of Fig. 12 and the insets are visual deductions from earlier diagrams. Symmetry with respect to  $u$  means  $u > 0$  same as  $u < 0$ .

The final set of pictures, Fig. 14-16, have except for a few well documented points a large element of visual deduction from previous figures and do not necessarily have the accuracy of the earlier diagrams. For these figures  $v$  is the missing variable.

## 5. Conclusions.

With this paper there are now fairly detailed pictures available for the discontinuity surface for all of Thom's seven elementary catastrophes. However, Thom himself has used cross-sections of the bifurcation surface of the parabolic umbilic (mark 2)

$$V = x^2y + (x^4 + y^4)/4 + ty^2 + wx^2 - ux - vy$$

in his book [3] and his later applications of the theory to the subject of linguistics. The diagrams corresponding to those of this paper for this new family of potentials show many interesting new features. The author hopes to present these in a subsequent paper.

$u = 0.0$

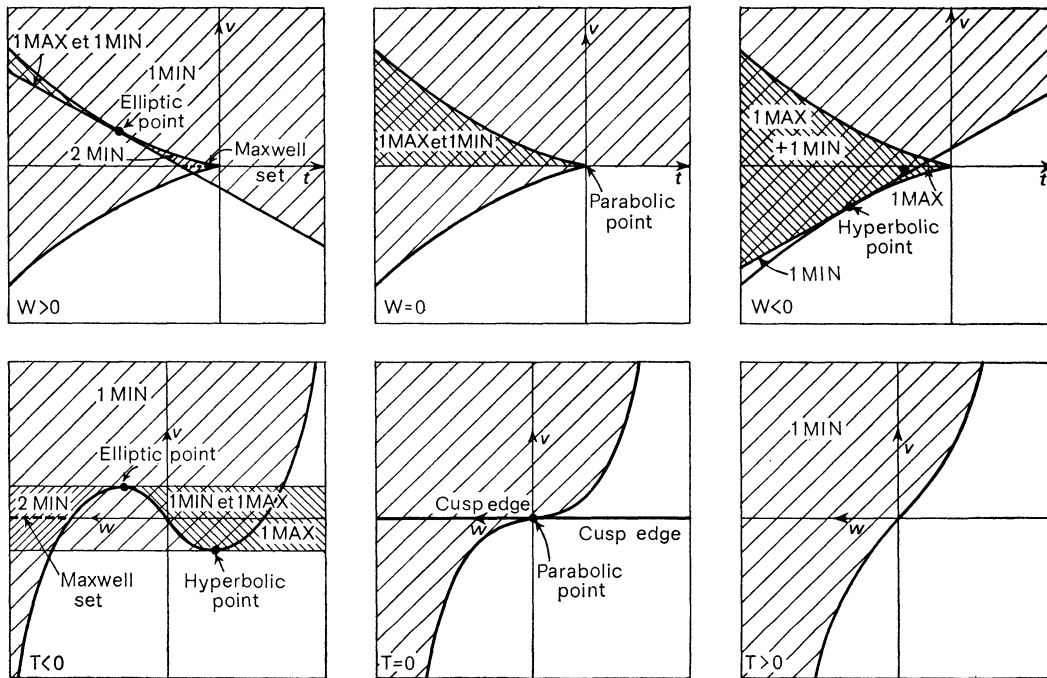
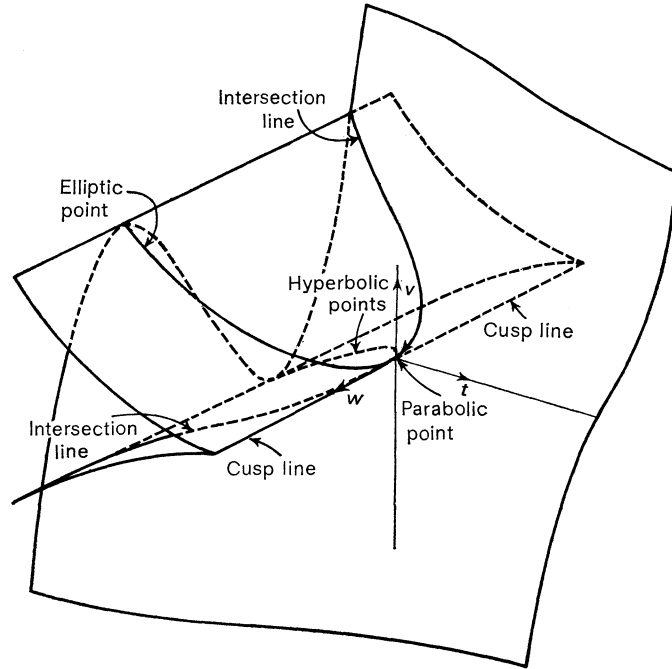


FIG. 12

$u \neq 0.0$

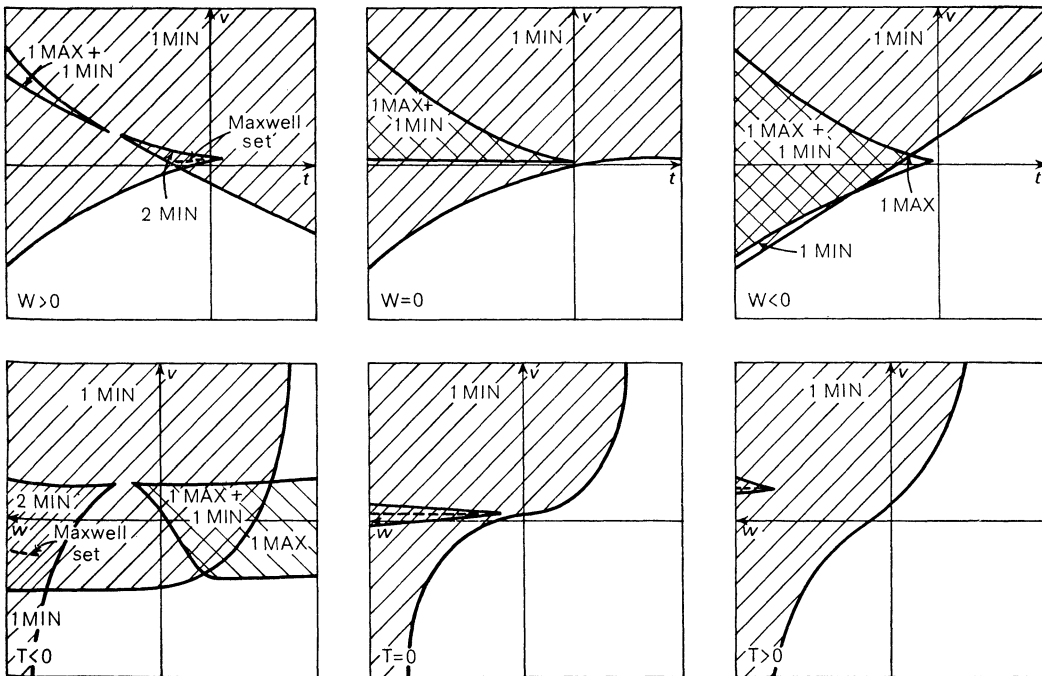
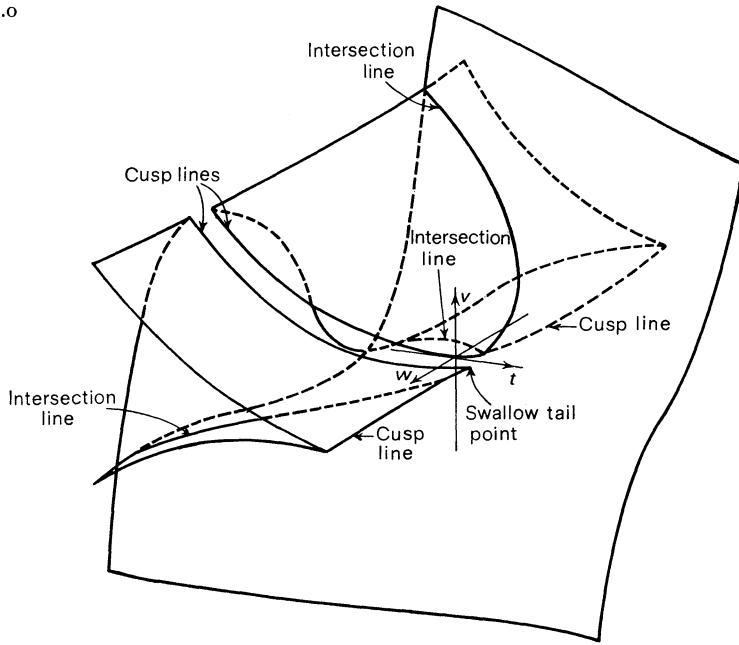


FIG. 13

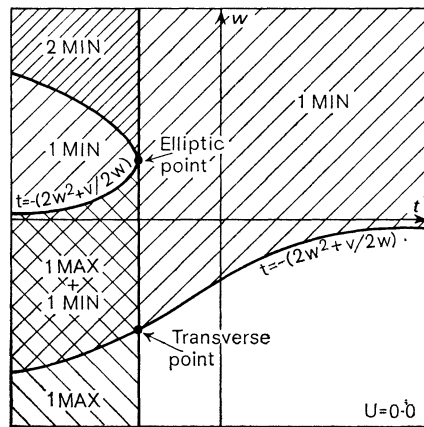
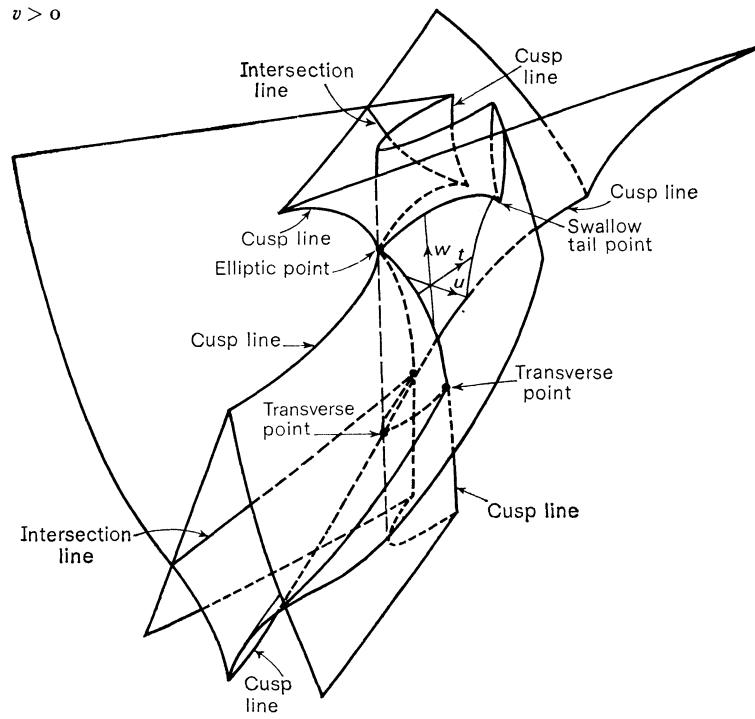


FIG. 14

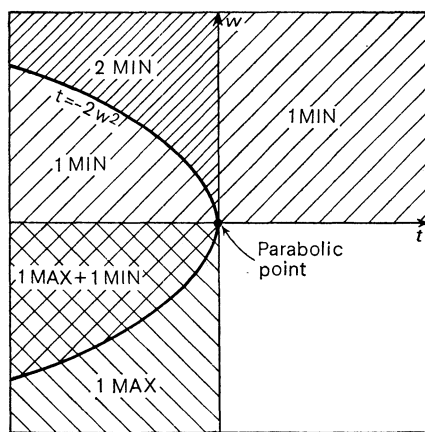
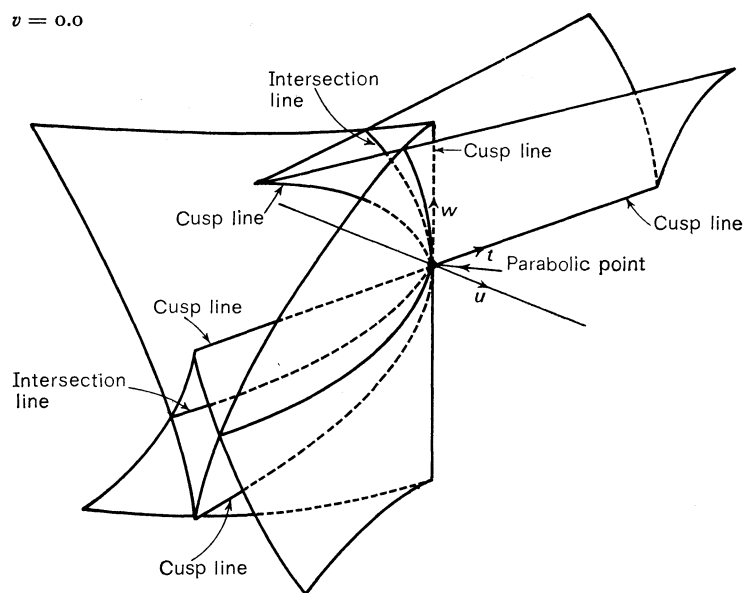


FIG. 15

$v < 0$

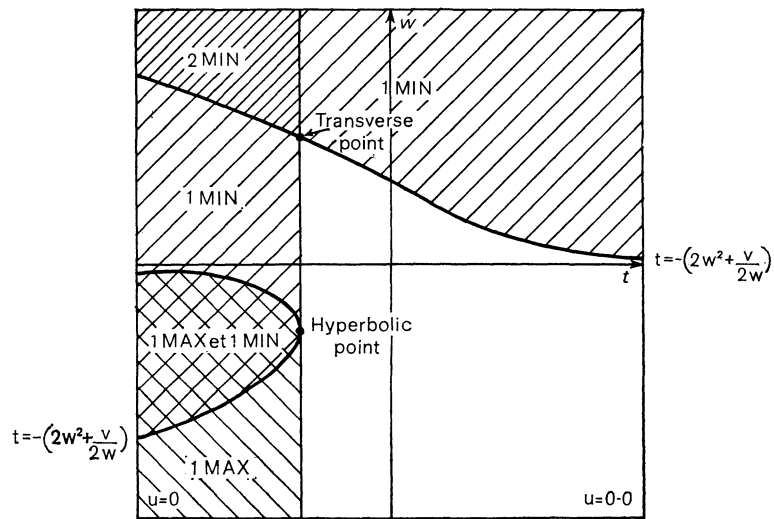
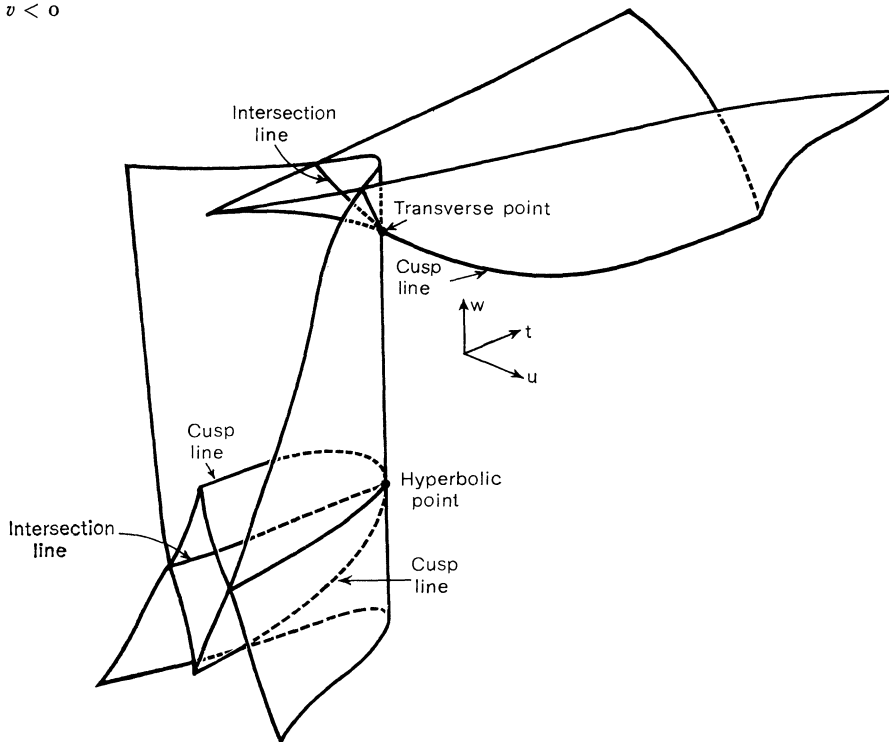


FIG. 16

**Acknowledgments.**

The author wishes to thank E. C. Zeeman for many helpful discussions of the work involved in this paper. He would also like to thank D. H. Fowler for useful comments on terminology and the referee for pointing out an error in Fig. 16 and for a very useful remark relating to improving the drawing of the Maxwell set.

Lanchester Polytechnic (Rugby Site), Eastlands, Rugby.

## REFERENCES

- [1] R. THOM, Topological Models in Biology, *Topology*, **8** (1969), 313-335.
- [2] R. THOM, Topologie et signification, *De Rham Commemorative*, Volume, Springer, 1970.
- [3] R. THOM, *Stabilité structurelle et morphogénèse*, Benjamin (to appear).
- [4] E. C. ZEEMAN, Breaking of Waves, *Proceeding of Symposium on Differential Equations and Dynamical Systems*, I, Maths. Institute, University of Warwick, 5.
- [5] E. C. ZEEMAN, Catastrophe Machines, *Proceedings of Liverpool Symposium on Singularities*, 1970 (to appear).

*Manuscrit reçu le 5 juin 1971.*